Spin dynamics in magnetic films patterned into dots and wires

J. Jorzick, S.O. Demokritov, B. Hillebrands
Fachbereich Physik and Schwerpunkt Materialwissenschaften, Universität Kaiserslautern, 67653 Kaiserslautern, Germany

B. Bartenlian, C. Chappert
IEF, Université Paris Sud, 91405 Orsay, France

F. Rousseaux
L2M, Baneux, France

A.N. Slavin
Department of Physics, Oakland University, Rochester, Michigan, USA

An experimental study of spin wave quantization in arrays of micron size magnetic $Ni_{80}Fe_{20}$ islands (dots and wires) by means of Brillouin light scattering spectroscopy is reported. Dipolar-dominated spin wave modes laterally quantized in a single island with quantized wavevector values determined by the size of the island are studied. In the case of wires the frequencies of the modes and the transferred wavevector interval, where each mode is observed, are calculated. The results of the calculations are in a good agreement with the experimental data. In the case of circular dots the frequencies of the lowest observed modes decrease with increasing distance between the dots, thus indicating an essential dynamic magnetic dipole interaction between the dots with small inter-dot distances.

1. Introduction

During the last decade patterned magnetic structures attracted a steeply increasing scientific interest. On one hand this is caused by recent progress achieved in lithographic techniques, which allows the fabrication of high quality, well-controlled, laterally defined magnetic structures. On the other hand it is driven by the miniaturization of high-speed, high-density, nonvolatile magnetic random access memory devices, where the application of magnetic structures like, e.g., dots and wires of micron or submicron sizes is very feasible [1,2]. However, increasing the memory density by scaling the bit sizes down to submicrometer sizes is not trivial, since the small size and high lateral density of the islands in an array affect their static and dynamic magnetic properties dramatically due to increasing magnetic dipole interaction between the bits. Although static properties of micron size magnetic dots and wires have been studied to some extent [3-6], their high-frequency dynamic properties, which are of great importance for high-speed optimization of possible devices, is just beginning [7-11].

The study of spin waves is a powerful method for probing the dynamic properties of magnetic media in general, and those of laterally patterned magnetic structures in particular. From spin wave measurements basic information on the magnetic properties, such as magnetic anisotropy contributions, the homogeneity of the internal field, as well as coupling between magnetic islands can be extracted. This information is often hard to obtain with other methods. In addition, spin waves, which are dynamic eigen-excitations, define the time scale of a magnetization reversal process, and, therefore, they are of fundamental importance to achieve an understanding of the time structure of the reversal. When the size of the object becomes comparable to the wavelength of a spin wave under investigation, quantization (or confinement) effects appear, which lead to dramatic changes in the spin wave spectrum and the spin-wave density of states. The spin wave quantization in magnetic wires differs from that in magnetic dots, since the former addresses the quantization of one component of the in-plane wavevector (perpendicular to the wire axis), whereas the latter the quantization of both components.

2. Spin wave spectrum of magnetic wires and dots

The problem of the calculation of a spin wave spectrum for an axially magnetized infinite ferromagnetic wire with a rectangular cross-section has never been solved analytically (see, e.g., comments in [12]). However, in a particular case of a thin wire described by $d << w$, where d is the thickness of the wire and w is its width, the spectrum of long-wavelength magnetic excitations can be calculated approximately using the theory of dipole-exchange spin waves in a magnetic film [13].

The dipole-exchange spin-wave spectrum in an infinitely extended ferromagnetic medium is given by the Herring-Kittel formula [14]

$$\nu = \frac{\gamma}{2\pi}\left[\left(H + \frac{2A}{M_S}q^2\right)\left(H + \frac{2A}{M_S}q^2 + 4\pi M_S \sin^2\theta_q\right)\right]^{1/2} \quad (1)$$

where γ is the gyromagnetic ratio, A is the exchange stiffness constant, $\vec{H}$ and $\vec{M}_S$ are the applied magnetic field and the saturation magnetization both aligned along the z-axis, $\vec{q}$ is the three-dimensional wavevector, and θ_q is the angle between the direction of the wavevector and the magnetization.

In a magnetic film with a finite thickness d the spin wave spectrum is modified due to the fact that the translational invariance is broken at the film surfaces. An approximate expression for spin wave frequencies of a film can be written in the form, analogous to Eq. (1) [13]:

$$\nu = \frac{\gamma}{2\pi}\left[\left(H + \frac{2A}{M_S}q^2\right)\left(H + \frac{2A}{M_S}q^2 + 4\pi M_S \cdot F_{pp}(q_\parallel d)\right)\right]^{1/2} \quad (2)$$

where

$$q^2 = q_y^2 + q_z^2 + \left(\frac{p\pi}{d}\right)^2 = q_\parallel^2 + \left(\frac{p\pi}{d}\right)^2 . \quad (3)$$

Here the normal to the film surface points along the *x*-direction. $q_\parallel$ is the continuously varying in-plane wavevector, F_{pp} ($q_\parallel$,d) is the matrix element of the magnetic dipole interaction, and p = 0,1,2,... is a quantization number for the so-called perpendicular standing spin waves (PSSW). Equation (3) is obtained for the dynamic part $\vec{m}$ of the magnetization under boundary conditions of "unpinned" spins on the film surfaces:

$$\left.\frac{\partial \vec{m}}{\partial x}\right|_{x=\pm d/2} = 0 . \quad (4)$$

If $\vec{q}_\parallel \parallel \vec{M}_S$, the dispersion equation for the lowest thickness mode (p = 0) can be derived from Eq. (2) neglecting exchange as follows [13]:

$$\nu = \frac{\gamma}{2\pi}\left[H\left(H + 4\pi M_S \cdot \frac{1-\exp(-q_\parallel d)}{q_\parallel d}\right)\right]^{1/2} \quad (5)$$

It is obvious from Eq. (5) that the frequency of the mode decreases with increasing wavevector, i.e., the group velocity of the mode is negative. This mode is known as a backward volume mode.

If $\vec{q}_\parallel \perp \vec{M}_S$, the dispersion equation for the lowest thickness mode (p = 0) calculated from Eq. (2) (for A = 0 as well) in the long wavelength limit coincides with that obtained from the Damon-Eshbach (DE) formula [15]:

$$\nu_{DE} = \frac{\gamma}{2\pi}\cdot\left[H\cdot(H + 4\pi M_s) + (2\pi M_s)^2 \cdot \left(1 - e^{-2q_\parallel d}\right)\right]^{1/2} . \quad (6)$$

In general, if the film is magnetized in plane, and if $\vec{q}_\parallel \perp \vec{M}_S$, the spin wave modes described by Eqs.(2) and (3) can be divided into the dipole dominated surface mode (p = 0) and exchange dominated, thickness- or perpendicular standing spin wave (PSSW) modes (p > 0). The frequency of the former is determined by Eq. (6), while the frequencies of the perpendicular standing modes (p > 0) can be approximately (in the long wavelength limit) calculated from the expression [13]:

$$\nu_p = \frac{\gamma}{2\pi}\left[\left(H + \frac{2A}{M_S}q_\parallel^2 + \frac{2A}{M_S}\left(\frac{p\pi}{d}\right)^2\right)\cdot\right.$$
$$\left.\left(H + \left[\frac{2A}{M_S} + H\left(\frac{4\pi M_s/H}{p\pi/d}\right)^2\right]q_\parallel^2 + \frac{2A}{M_S}\left(\frac{p\pi}{d}\right)^2 + 4\pi M_S\right)\right]^{\frac{1}{2}} \quad (7)$$

It is clear from Eq. (7) that the $n_p(q_\parallel)$ dependence is rather weak for $q_\parallel << pp/d$. In the general case, when exchange and mode hybridization effects are important, the numerical approach is usually used for the determination of the spin wave frequencies in films [16].

If we consider a magnetic wire magnetized in plane along the *z*-direction and having a finite width *w* along the *y*-direction as shown in Fig. 1a, a boundary condition similar to Eq. (4) at the lateral edges of the wire should be imposed:

$$\left.\frac{\partial \vec{m}}{\partial y}\right|_{y=\pm w/2} = 0 \quad (8)$$

An additional quantization of the *y*-component of $\vec{q}_\parallel$ is then obtained:

$$q_{y,n} = \frac{n\pi}{w} \quad (9)$$

where n = 0,1,2,... . Using Eqs. (6) and (7) and the quantization expression (9) one can calculate the frequencies of width- (or laterally quantized) modes. The profile of the dynamic part of the magnetization $\vec{m}$ in the *n*-th mode can be written as follows:

$$\vec{m}_n(y) = \vec{a}_n \cdot \cos\left(q_{y,n}\left(y + \frac{w}{2}\right)\right), \; -\frac{w}{2} < y < \frac{w}{2} \quad (10)$$

Equation (10) describes a standing mode consisting of two counterpropagating waves with quantized wavevectors, $q_{y,n}$. Note here, that due to the truncation of the cosine function at the wire boundaries, the quantized values $q_{x,p}$ and $q_{y,n}$ are not true wavevectors.

The theoretical modeling of the spin wave spectrum in magnetic dots faces even more difficulties than the modeling for the wires. The problem is obviously connected to the two-dimensional origin of spin wave confinement in discs. Earlier experimental studies of the magnetostatic modes of *tangentially* magnetized macroscopic discs using a ferromagnetic resonance technique [17] do not present any comparison of the experimental findings with the theory. Surprisingly, despite numerous publications on inhomogeneous magnetostatic modes in finite-size magnetic samples (see, e.g., [18] and references therein) there is no appropriate theoretical description of such modes up to now. This can be probably explained by the low symmetry of the problem. In fact, in his pioneering work, Walker [19] considered an *axially* magnetized spheroid. The direction of the in-plane magnetization of the *tangentially* magnetized dot breaks the axial symmetry of the Walker equation [20]. The solution (analytical or numerical) of the Walker equation, corresponding to a tangentially magnetized disc is still needed. However, a qualitative analysis of the mode frequencies in a tangentially magnetized circular dot shows that there are non-uniform modes with frequencies both higher and lower than the frequency of the uniform mode, as follows. For large wavevectors, when the lateral confinement is not important, the modes converge to spin waves in an infinite film. Here there exist two types of spin wave modes: the Damon-Eshbach modes ($\vec{q}_\parallel \perp \vec{M}$) with a positive group velocity and the backward volume modes ($\vec{q}_\parallel \parallel \vec{M}$) with a negative group velocity. Therefore, there can exist modes in a dot with their frequencies below and above the frequency of the uniform mode depending on their main in-plane direction, along which the corresponding wavenumber is largest.

There are very few studies of the dynamic properties of magnetic dots and wires. In early investigations of BLS from spin waves in an array of permalloy wires Gurney et al. [21] have observed a splitting of the spin wave spectrum into several discrete modes. However, the authors were not able

to identify the nature of the modes. Very recently Mathieu et al. [7] investigated spin wave in arrays of permalloy wires by BLS. In addition to demagnetization effects a quantization of the spin wave mode in several dispersionless modes, caused by a confinement effect of the spin waves, was observed and quantitatively described [7]. Cherif et al. [22] studied magnetic properties in periodic arrays of square permalloy dots. The spin wave frequencies were found to be sensitive to the size of the dots and, for the smallest structures, to the in-plane direction of the applied field. Hillebrands et al. [9,23] investigated spin wave properties of square lattices of micron-sized dots of permalloy with varying dot separations. They have found a fourfold anisotropy which is caused by a magneto-dipole interaction between residual magnetically unsaturated parts of the dots.

3. Experimental procedure

Our samples are made of permalloy ($Ni_{80}Fe_{20}$) films with thicknesses *d* of 10, 20 and 40 nm deposited in UHV onto a Si (111) substrate by means of e-beam evaporation. The films were covered by Pd or Cr overlayers to prevent oxidation. Static magneto-optic Kerr-effect (MOKE) measurements on the non-patterned films demonstrated a high quality of the films documented by a very low (< 5 Oe) induced in-plane magnetic anisotropy. After being tested, the films were patterned to create two-dimensional square arrays of circular dots or arrays of wires. Patterning was performed using X-ray lithography. The patterning masks were fabricated by means of a JEOL 5D2U nanopattern generator at 50 keV. X-ray exposure was performed at the super-ACO facility (LURE, Orsay, France) using a negative resist and a liftoff process with Al coating and ion milling [24]. Different samples with various combinations of dot diameters (D = 1 and 2 μm), dot thicknesses (d =10, 20, 40 nm) and dot separations (δ = 0.1, 0.2, 1 and 2 μm) as well as wire arrays with wire thicknesses of 20 and 40 nm, a wire width of 1.8 μm and distances between the wires of 0.7 μm and 2.2 μm were prepared. The overall dimensions of the arrays were $500\times500\mu m^2$. Figures 1a and 1b present a scanning electron microscope images of two arrays of magnetic wires with the same wire widths but with different distances between the wires and four patterning dot layouts, respectively. The used technique guarantees a high-quality patterning process, which provides a superb flatness of the wire boundaries and excellent reproducibility of the dot shapes. An investigation of the magnetization reversal behavior of the structures, performed by MOKE magnetometry, showed that the magnetic easy axis of the wire array was along the wire axis, which is expected from magnetic shape anisotropy considerations.

a)

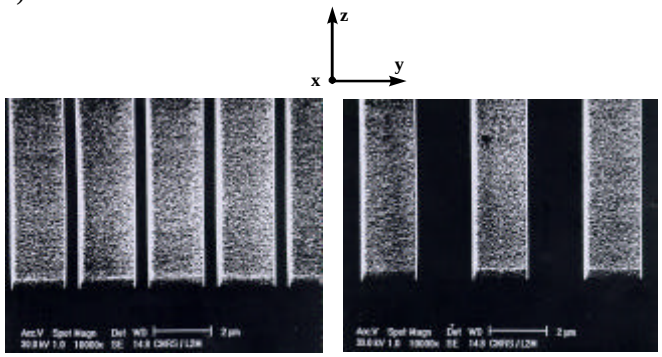

b)

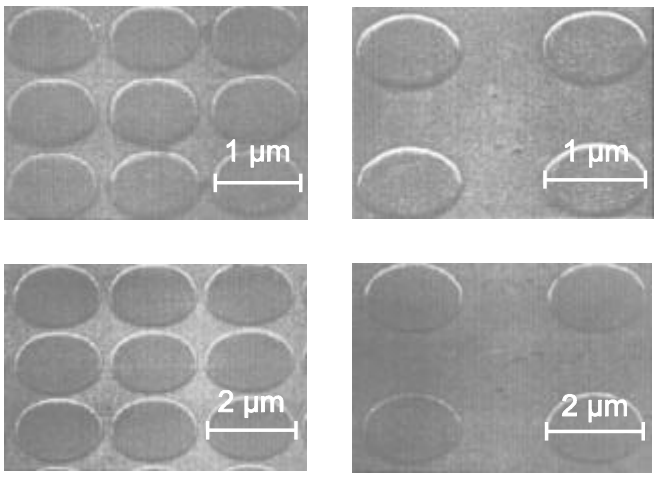

Fig. 1: a) SEM micrographs of the wires under investigation. The orientation of the Cartesian coordinate system used for calculations is shown as well. b) SEM micrograph of the investigated dot arrays. Due to the oblique incidence of the electron beam the circular dots appear ellipsoidal.

The spin wave properties were investigated at room temperature by means of BLS in a backscattering geometry using a computer controlled tandem Fabry-Perot interferometer which is described elsewhere [25]. BLS is used since a long time for the investigation of spin waves in thin magnetic films and layered structures [26, 27]. However, this technique is particularly well suited for the investigation of spin waves in laterally patterned systems. The main advantages of BLS are its high spatial resolution defined by the size of the laser beam focus, which is 30-50 μm in diameter, and the possibility to investigate spin waves with different absolute values and orientations of their wavevectors, $\vec{q}_{\parallel}$. The former circumstance allows one to investigate small pattern areas, which simplifies the patterning procedure. Performing the BLS experiment with different $\vec{q}_{\parallel}$ one can obtain the information of the spatial distribution of the magnetization $\vec{m}$ in a laterally confined island (dot or wire), and one can identify the spin wave mode unambiguously.

Laser light of a single moded, frequency stabilized (Dn = 20 MHz) Ar^+ laser with a wave length of l_{laser} = 514.5 nm and a laser power of 50 mW was focused onto the sample and the frequency spectrum of the backscattered light was analyzed. An external field was applied either along the wires or along the axis of the dot lattice, while the in-plane wavevector $\vec{q}_{\parallel} = (\vec{q}_S - \vec{q}_I)_{\parallel}$, transferred in the light scattering process, was oriented perpendicular to the applied field, and its value was varied by changing the angle of light incidence, θ, measured from the surface normal: $q_{\parallel} = (4\pi/l_{Laser})\cdot\sin\theta$.

For identification of the spin wave modes in wires the BLS scattering cross section of a given mode was measured. Due to a possible variation over time in the transmission of the interferometer during the course of measurements, it is, in general, very difficult to measure absolute values of the BLS scattering cross section. To overcome this problem, we used the PSSW mode, registered for the entire investigated range

of $q_{||}$, as a reference for relative measurements of the BLS scattering cross section. The BLS intensity corresponding to each in-plane mode was normalized to the intensity of the PSSW mode. The relative intensities obtained in this way are very reproducible and were used for measuring the lateral distribution of the dynamic magnetization through the wire using the approach discussed above.

4. Results and discussion: wires

Figure 2 shows a typical BLS spectrum for the sample with a wire width of 1.8 µm and a separation between the wires of 0.7 µm. A transferred wavevector $q_{||} = 0.3 \cdot 10^5$ cm^{-1} was oriented perpendicular to the wires, while an external field of 500 Oe was applied along the wire axis. As it is seen in Fig. 2, the spectrum contains four distinct modes near 7.8, 9.3, 10.4, and 14.0 GHz. Note here, that in the region of interest (5-17 GHz) the scanning speed of the interferometer was reduced by a factor of three to increase the accumulation time in this region and, thus, to improve the signal-to-noise ratio. By varying the applied field the spin wave frequency for each mode was measured as a function of the field, as displayed in Fig. 3. The observed dependence of all frequencies on the field confirms that all detected modes are magnetic excitations.

To identify the nature of the observed modes, the dispersion of the modes was measured by varying the angle of light incidence, θ, and, thus the magnitude of the transferred wavevector, $q_{||}$. The results are displayed in Fig. 4 for two samples with the same wire thickness of 40 nm and width of 1.8 µm, but with different wire separations of 0.7 µm (open symbols) and 2.2 µm (solid symbols). It is clear from Fig. 4 that one of the detected modes, presented by circles, (near 14 GHz) is the PPSW mode, corresponding to $p = 1$ in Eq. (7). In the region of low wavevectors the spin wave modes show a disintegration of the continuous dispersion of the Damon-Eshbach mode of an infinite film into several discrete, resonance-like modes with a frequency spacing between the lowest lying modes of approximately 0.9 GHz for $d = 20$ nm (not shown) and 1.5 GHz for $d = 40$ nm. As it is clear from Fig. 4, there is no significant difference between the data for the wires with a separation of 0.7 µm and 2.2 µm. This fact indicates that the mode splitting is purely caused by the quantization of the spin waves in a single wire due to its finite width.

As it is seen in Fig. 4, the first PPSW mode ($p = 1$) was observed in the arrays with a wire thickness of 40 nm for the entire investigated range of $q_{||}$. It was used as a reference for relative measurements of the BLS scattering cross section, as it was described above. The results of these measurements are shown by black squares in Fig. 5.

Having a more close look on the dispersion curves and the BLS cross section profiles of the magnetic wires one can summarize the main features as follows: (i) For low wavevector values ($0 - 0.8 \cdot 10^5$ cm^{-1}) the discrete modes do not show any noticeable dispersion, behaving like standing wave resonances. (ii) Each discrete mode is observed over a continuous range of the transferred wavevector $q_{||}$. (iii) The lowest two modes appear very close to zero wavevector, the higher modes appear at higher values. (iv) The frequency splitting between two neighbored modes is decreasing for increasing mode number. (v) There is a transition regime ($q_{||} = 0.8 - 1.0 \cdot 10^5$ cm^{-1}) where the well resolved dispersionless modes converge towards the dispersion of the continuous film (see dashed lines in Fig. 4). (vi) There is no noticeable difference for the samples with the same wire width w but different wire separations (0.7 µm and 2.2 µm).

In order to understand the above experimental findings we need (i) to explain why each discrete mode is observed over a characteristic continuous range of transferred wavevectors, and (ii) to calculate the frequencies of the observed eigenmodes.

Since the discrete, dispersionless spin wave modes observed for small wavevectors converge towards the dispersion of the DE mode of the continuous film, it is natural to assume that these modes result from a width dependent quantization of the in-plane wavevector of the DE mode, discussed above. As it was shown, the profile of the dynamic part of the magnetization m in the n-th mode has a cosine-like shape (see Eq. (10)). The analysis performed in [28] shows that the light scattering intensity $I_n(q)$ for each standing lateral mode is proportional to the Fourier transform m_q squared. Due to the truncation of the cos-function at the boundaries of the

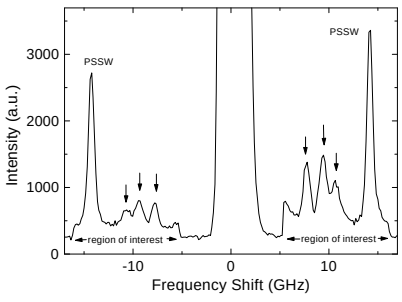

Fig. 2: Experimental Brillouin light scattering spectra obtained from the sample with a thickness of 40 nm, a wire width of 1.8 µm and separation of the wires of 0.7 µm. The applied field was 500 Oe orientated along the wire axis and the incoming wavevector of the light was orientated perpendicular to the wires. The transferred wavevector was $q_{||} = 0.3 \cdot 10^5$ cm^{-1}. In the region of interest (5-17 GHz) the scanning speed was reduced by a factor three increasing the number of recorded photons by the same factor. The arrows indicate the in-plane quantized spin wave modes.

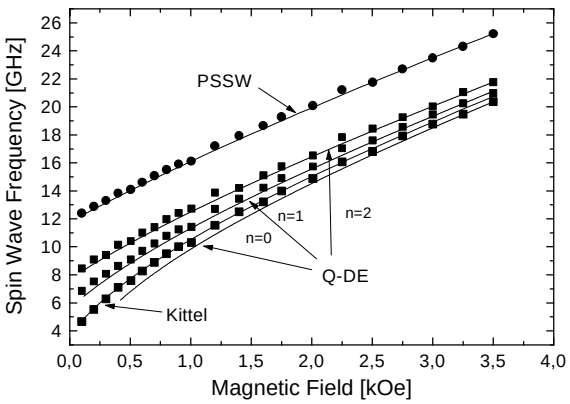

Fig. 3: Frequencies (for $q_{||} = 0.3 \cdot 10^5$ cm^{-1}) of the in-plane quantized spin wave modes of the wire array with a wire width of 1.8 µm and a wire thickness 40 nm as a function of the applied field. The lines are calculated using either the DE-equation with quantized wavevectors (Q-DE) or the Kittel formula (Eq. (11)) as indicated. The line labeled PSSW shows the frequency of the first perpendicular standing spin wave calculated using a numerical procedure [12].

wire, m_q is non-zero over a continuous interval of q and, thus, the discrete modes are observed over a finite interval of the transferred wavevector $q_{||}$. The results of this calculation for the lowest five modes, normalized for the best fit of the $n = 0$ mode, are shown in Fig. 6b by gray colored lines. A good agreement between the experimental data and the results of the calculation justifies the chosen boundary condition and confirms that the observed spin wave modes are in fact the quantized DE modes.

The frequencies of the observed modes can be approximately determined by substituting the obtained quantized values of wavevector, $q_{y,n}$, into the dispersion equation of the DE mode, Eq. (6). The results of these calculations are shown in Fig. 4 by the solid horizontal lines. For the calculation the geometrical parameters (wire thickness d = 40 nm, wire width w = 1.8 µm) and the independently measured material parameters $4\pi M_s$ = 10.2 kG and $\gamma/2\pi$ = 2.95 GHz/kOe were used. Without any fit parameters the calculation reproduces all mode frequencies with $n > 0$ very well, and for the $n = 0$ mode a reasonable agreement is achieved. Since the group velocity $V_g = 2\pi\partial\nu/\partial q$ of the dipolar surface spin wave (cf. Eq. (6)) decreases with increasing wavevector, the frequency splitting of neighboring, width-dependent discrete spin wave modes, which are equally spaced in q-space ($q_{y,n} = n\pi/w$), becomes smaller with increasing wavevector $q_{y,n}$, until the mode separation is smaller than the frequency resolution in the BLS experiment and/or the natural line width, and the splitting is no longer observable in Fig. 4. The evolution of the mode frequencies with an increasing applied field, as illustrated in Fig. 3, can be described as well. The solid lines marked as "Q-DE" are calculated using Eq. (6) with the quantized values of wavevector. With the exception of the curve for $n = 0$ they also demonstrate a very good agreement with the experiment.

Although the spatial distribution and the frequencies of the observed modes are well reproduced, the above approach ignores the correction of dynamic dipole fields due to the finite width of the wires. Since the magnetic dipole interaction is a long-range one, the strength of the field at a given position is determined not only by the amplitude of the dynamic magnetization in the vicinity of this position, but also by the spatial distribution of the dynamic magnetization far from this position. Therefore, due to finite size effects caused by the side walls, the dipole fields accompanying a quantized mode in the wire differ from those of the DE-mode of the infinite film with the same wavevector. This correction, which is small in any case for the wires with a high aspect ratio, is negligible for all modes with sufficiently high quantum numbers (i.e., for modes with either p or n larger than zero). It is, however, observable for the lowest, uniform mode ($p = 0$, $n = 0$). The finite size effect can be easily taken into account for long wires with ellipsoidal cross-section since the dynamic dipole field is homogeneous in this case. The corresponding frequency is given by the Kittel-formula [29]:

$$\nu = \frac{\gamma}{2\pi}\cdot\left[\left(H + N_x\cdot 4\pi M_S\right)\cdot\left(H + N_y\cdot 4\pi M_s\right)\right]^{1/2} \qquad (11)$$

where N_x and are the demagnetization factors along the x- and y-direction in the wire cross-section (note here that the demagnetization factor along the wire, N_z, is negligible). In our particular case of a wire with a rectangular cross-section Eq. (11) is not exactly applicable, as the dynamic demagnetization field is not exactly homogeneous. However, since the thickness of the wire is much smaller than its width ($d << w$), one can consider this field to be approximately homogeneous in agreement with the analytical solution for demagnetizing fields of a rectangular prism found by Joseph and Schlömann [30]. The corresponding demagnetization factors are: $N_y = 2d/\pi w$, $N_x = 1 - N_y$. The calculated value of N_y is in a good agreement with that obtained from static measurements. The frequency of the lowest mode calculated on the basis of Eq. (11) using the above demagnetization factors is shown by a dotted horizontal line in Fig. 4. Its field dependence is illustrated in Fig. 3 by a solid line, marked as "

The agreement with the experiment is convincing. It is much more complicated to take into account the finite size effects

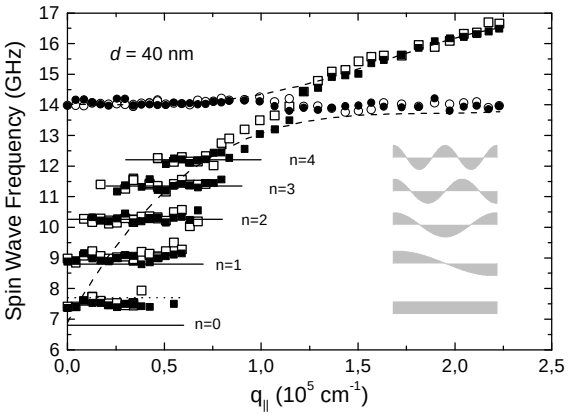

Fig. 4: Obtained spin wave dispersion curves for an array of wires with a wire thickness of 40 nm, a wire width of 1.8 µm and a separation between the wires of 0.7 µm (open symbols) and 2.2 µm (solid symbols). The external field applied along the wires axis was 500 Oe. The solid horizontal lines indicate the results of a calculation using Eq. (6) with the quantized values of $q_{||}$. The dotted horizontal line indicates the result of calculations for the mode $n = 0$ using Eq. (11). The dashed lines showing the hybridized dispersion of the Damon-Eshbach mode and the first perpendicular standing spin wave mode were calculated numerically for a continuous film with a thickness of 40 nm. On the right side the mode profiles are illustrated.

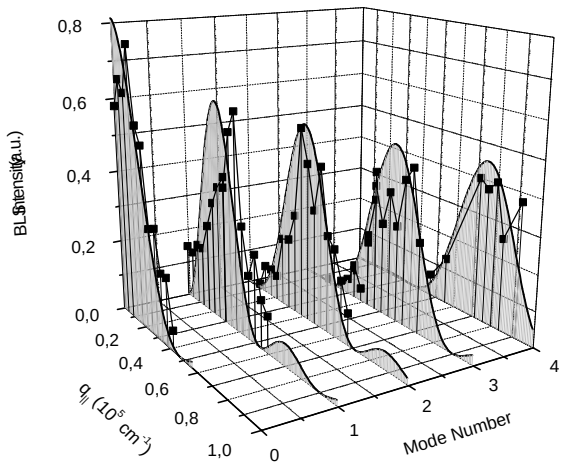

Fig. 5: Measured BLS intensities (black squares), normalized to the intensity of the PSSW mode, of the in-plane quantized spin wave modes as a function of the wavevector $q_{||}$ and the mode number n in comparison to the calculated Fourier transform m_q squared (gray colored curves).

for the non-uniform modes. However, from the qualitative considerations it is obvious that the correction of the demagnetizing fields (or demagnetization factors) due to the finite size of the wire rapidly decreases with increasing mode number. Therefore, the good reproduction of the mode frequencies for $n > 0$ just on the basis of Eq. (6) is not surprising.

5. Results and discussion: circular dots

Figure 6 shows the anti-Stokes side of a typical Brillouin light scattering spectrum for a transferred wavevector of $q_{||} = 0.21 \cdot 10^5$ cm^{-1} for the sample with a dot thickness of 40 nm, a dot diameter of 2 µm, and a dot separation of 0.2 µm. An external field of 600 Oe was applied in-plane along the array axis. Near 7.0, 7.9, 9.8, 11.4 and 14 GHz several distinct spin wave modes are clearly observed. All these modes are magnetic excitations as concluded from the measured field dependence of the mode frequencies. The peak near 14 GHz is also observed on the non-patterned films. It has a dot thickness dependence $w \propto d^{-2}$, and it shows no essential Stokes/anti-Stokes asymmetry. Therefore, it is identified as corresponding to the perpendicular standing exchange dominated spin wave mode. The value of the exchange stiffness, calculated from the measured frequencies of these modes is $A = 1 \cdot 10^{-6}$ erg/cm, which is in a good agreement with the results of other studies [31].

By changing the angle of light incidence the value of $q_{||}$ is varied and the dispersion of the observed mode is obtained as demonstrated in Fig. 7 for the array of dots with 2 µm dot diameter and 0.2 µm dot separation. As it is seen in the figure, several discrete dispersionless modes are detected over the measured wavevector interval. A tendency that the splitting between neighboring modes decreases with increasing mode frequencies is clearly seen. A similar effect has already been observed for magnetic wires. It is due to the fact that the group velocity $V_g = \partial\omega/\partial q$ of the Damon-Eshbach mode decreases with increasing wavevector. In the case of wires, where the spin wave modes are characterized by quantized equidistant wavenumbers $q_{||,i}$, this fact necessarily leads to a decreasing frequency splitting. Two-dimensional quantization conditions in a circular dot are not so simple, as are those for the wires. Therefore, it is not surprising that the splitting between the three lowest lying modes, shown in Fig. 7, presents an exception from this rule.

Using a numerical procedure [16], the frequencies of the Damon Eshbach mode and the first perpendicular standing spin wave mode for an infinitely extended, continuous film of same thickness (d = 40 nm) were calculated, using the values of the demagnetizing factors, obtained from separate static MOKE magnetometry. The results of the calculation are plotted in Fig. 7 as dashed lines. The frequency of the uniform mode of a single disc (ω = 7.35 GHz) calculated using the Kittel-formula [29], is shown as a horizontal dotted line as well. The calculations clearly demonstrate that for large transferred wavevectors ($2\pi/q_{||} << D$) the measured dispersion converges to the dispersion of a continuous film of the same thickness, and the two quantized lowest modes have frequencies near the frequency of the uniform mode.

The five lowest spin wave modes of arrays of dots with the same dot thickness as presented in Fig. 7, but with a smaller dot diameter (D = 1 µm) are shown in Fig. 8 for two different dot spacings. First, it is clear from a comparison of Figs. 7 and 8, that the wavevector interval, where each mode is observed, scales approximately as D^{-1}. This result is in agreement with the theoretical analysis performed in [28], which has shown that the light scattering intensity from a given spin wave mode confined in an island is determined by the Fourier transform of the mode profile over the island. Second, changing the thickness of the dots, one observes that the frequency splitting between neighboring modes decreases with decreasing dot thickness, in accordance with the fact that the group velocity of the Damon-Eshbach mode at a given $q_{||}$ decreases with decreasing film thickness. The above presented experimental findings lead to the conclusion that the observed dispersionless, resonance-like modes are the spin waves, quantized due to lateral confinement in a single dot. As it was already mentioned, there is no theory describing the spectrum of spin waves confined in a tangentially magnetized circular dot. However, the obtained results

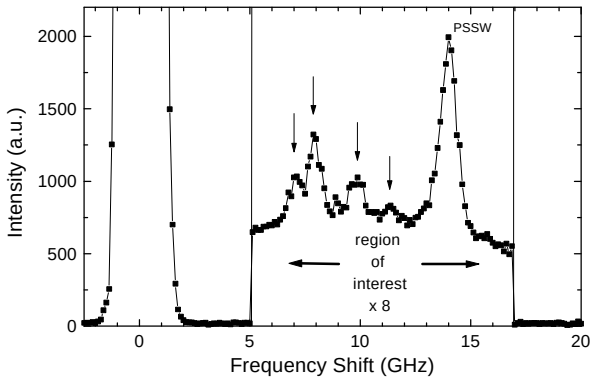

Fig. 6: Obtained BLS spectrum for a sample with a dot diameter of 2 µm and a dot separation of 0.2 µm for $q_{||} = 0.21 \cdot 10^5$ cm^{-1} with an external field of 600 Oe applied in-plane demonstrating the existence of several discrete spin wave modes. The peaks corresponding to laterally quantized modes are indicated by arrows. In the "region of interest" the scanning speed was reduced by a factor of eight, increasing the number of photon counts by this factor. At zero frequency shift the peak of the elastically scattered light appears.

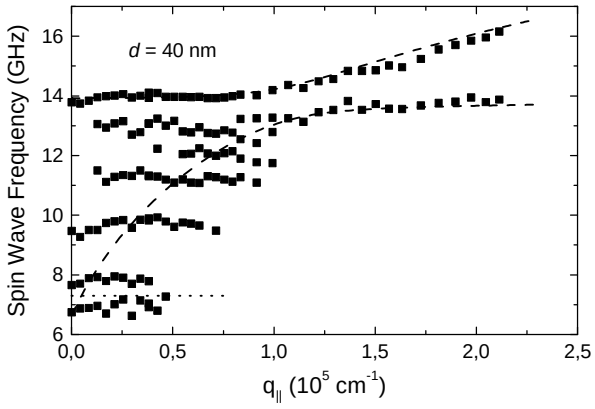

Fig. 7: Obtained spin wave dispersion curve for a square array of dots with a dot thickness of 40 nm, a dot diameter of 2 µm and a dot separation of 0.2 µm. An external field of 600 Oe was applied in-plane along the axis of the array lattice. The dashed lines show the results of a spin wave calculation for a continuous film of the same thickness as the dots. The dotted line marks the calculated frequency of the uniform mode of a single dot.

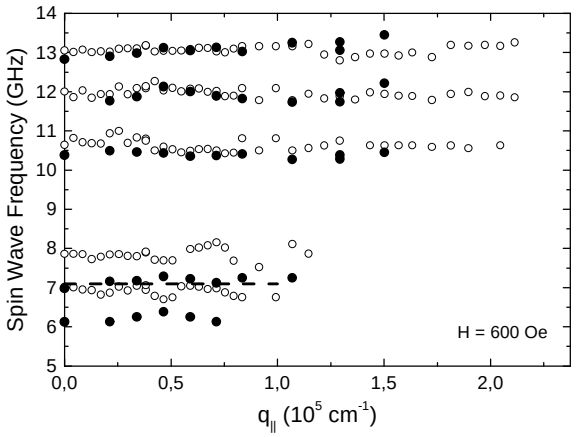

Fig. 8: Dispersion of the five lowest spin wave modes measured on a square array of dots with a dot thickness of 40 nm and a dot diameter of 1 µm. An external field of 600 Oe was applied in-plane along the axis of the array lattice. Open symbols indicate data for a dot separation of 0.1 µm, full symbols of 1 µm. The dot horizontal line indicates the calculated frequency of the uniform mode of a single dot.

are in an agreement with the qualitative considerations presented above.

Since the considered spin waves are the magnetostatic modes, and since magnetic dipole interaction is long-range, the question of a possible inter-dot mode coupling is of importance. Also, from the practical point of view, inter-dot coupling restricts the density of dot arrays in, e.g., magnetic memory applications. Figure 8 shows the frequencies of the spin wave modes, obtained on arrays having the same dot thicknesses and dot diameter, but with different inter-dot distances: open symbols correspond to δ = 0.1 µm, whereas full symbols correspond to δ = 1 µm. A clear frequency upshift of the two lowest modes of the sample with δ = 0.1 µm documents the existing inter-dot mode coupling. The weaker influence of the inter-dot coupling on higher modes can be understood as follows: Higher modes have mode profiles with a high number of nodes. The dynamic dipole field created by such profiles outside the dot is weaker compare to those of the homogeneous mode. Therefore the dynamic inter-dot mode coupling caused by those fields is weaker.

As a final remark, let us emphasize the difference between the lateral spin wave quantization observed in this work and the quantization of perpendicular standing spin waves in thin magnetic films. The former effect is the quantization of the dipole dominated spin waves with relatively small in-plane wavevectors and with frequencies determined by long-range interacting dipole fields, whereas the latter describes spin waves with large wavevectors perpendicular to the film plane, defined by the thickness of the film and with frequencies determined by the exchange stiffness. Due to the long-range nature of the dipole fields, laterally quantized spin waves can form collective excitations under appropriate conditions in arrays of wires. Investigations of such collective excitation are the subject of future studies.

In summary, we have observed spin wave quantization in a periodic array of magnetic dots and wires. The discrete modes can be understood as the width-dependent quantization of the dipolar surface spin wave mode (in-plane quantized DE mode). In the case of wires an excellent agreement between the calculated and measured values of (i) the frequency of the modes, (ii) the wavevector interval, where the modes are observed, and (iii) the BLS-intensity vs. wavevector dependence of each mode support our interpretation. For larger wavevectors quantized modes converge towards the dispersion of the infinite continuous film. The spin wave modes quantized in circular dotes are studied for samples with different dot diameters and thicknesses, as well as with different inter-dot distances. The existence of inter-dot mode coupling is found. For a full description of the frequencies and the mode profiles of the dots further theoretical work is required.

Support by the Deutsche Forschungsgemeinschaft, the European Community network “Dynaspin”, and the National Science Foundation (Grant DMR-9701640) is gratefully acknowledged.

References

[1] W.J. Gallagher, S.S.P. Parkin, Y.Lu, X.P. Bian, A. Marley, K.P: Roche, R.A. Altman, S.A. Rishton, C. Jahnes, T.M. Shaw, G. Xiao, J. Appl. Phys. 81, 3741(1997).

[2] S.S.P. Parkin, K.P. Roche, M.G. Samant, P.M. Rice, R.B. Beyers, R.E. Scheuerlein, E.J. O’Sullivan, S.L. Brown, J. Bucchigano, D.W: Abraham, Yu Lu, M. Rooks, P.L. Trouilloud, R.A. Wanner, and W.J. Gallagher, J. Appl. Phys. 85, 5828 (1999).

[3] J.F. Smyth, S. Schultz, D.R. Fredkin, D.P. Kern, S. A. Rishton, H. Schmid, M. Cali, and T. R. Koehler, J. Appl. Phys. 69, 5262 (1991).

[4] A. Maeda, M. Kume, T. Ogura, K. Kukori, T. Yamada, M. Nishikawa, and Y. Harada, J. Appl. Phys. 76, 6667 (1994).

[5] N. Bardou, B. Bartenlian, F. Rousseaux, D. Decanini, F. Carcenac, E. Cambril, M.-F. Ravet, C. Chappert, P. Veillet, P. Beauvillain, R. Megy, W. Geerts, and J. Ferre, J. Magn. Magn. Mater. 148, 293 (1995).

[6] A.O. Adeyeye, J.A.C. Bland, C. Daboo, J. Lee, U Ebels, and H. Ahmed, J. Appl. Phys. 79, 6120 (1996).

[7] C. Mathieu, J. Jorzick, A. Frank, S.O. Demokritov, A.N. Slavin, B. Hillebrands,
B. Bartenlian, C. Chappert, D. Decanini, F. Rousseaux, and E. Cambrill, Phys. Rev. Lett. 81, 3968 (1998).

[8] A. Ercole, A.O. Adeyeye, J.A.C. Bland, and D.G. Hasko, Phys. Rev. B 58, 345 (1998).

[9] C. Mathieu, C. Hartmann, M. Bauer, O. Büttner, S. Riedling, B. Roos, S.O. Demokritov, B. Hillebrands, B. Bartenlian, C. Chappert, D. Decanini, F. Rousseaux, A. Müller, B. Hoffman, U. Hartmann, Appl. Phys. Lett. 70, 2912 (1997).

[10] A. Ercole, A.O. Adeyeye, C. Daboo, J.A.C. Bland, D.G. Hasko,. J. Appl. Phys. 81, 5452 (1997).

[11] M. Grimsditch, Y Jaccard, I.K. Schuller, Phys. Rev. B 58, 11539 (1998).

[12] A.G. Gurevich and G.A. Melkov, *Magnetization Oscillations and Waves*, CRC Press, New York, 1996.

[13] B.A. Kalinikos and A.N. Slavin, J. Phys. C: Solid State Phys. 19,7013 (1986).

[14] C. Herring and C. Kittel, Phys. Rev. 81, 869 (1951).

[15] R.W. Damon and J.R. Eshbach, J. Phys. Chem. Solids 19, 308 (1961).

[16] B. Hillebrands, Phys. Rev. B 37, 8885 (1988); B. Hillebrands, Phys. Rev. B 41 530 (1990).

[17] J.F. Dillon, J. Appl. Phys. 31, 1605(1960).

[18] R.D. McMichael, P.E. Wigen, Magnetostatic spin modes in thin films, in: P.E. Wigen (ed.), “Nonlinear Phenomena and Chaos in Magnetic Materials“, World Scientific, Singapore, 1994.

[19] L.R. Walker, Phys. Rev. 105, 390 (1957).

[20] J.F. Dillon, H. Kamimura, J.P. Remeika, J. Appl. Phys. 34, 1240 (1963).

[21] B.A. Gurney, P. Baumgart, V. Speriosu, R. Fontana, A. Patlac, T. Logan, and P. Humbert, Digest of the International Conference on Magnetic Films and Surfaces, P7.12, p. 474, Glasgow (1991).

[22] S.M. Cherif, C. Dugautier, J.-F. Hennequin, P. Moch, J. Magn. Magn. Mater. 175, 228 (1997).

[23] B. Hillebrands, C. Mathieu, M. Bauer, S.O. Demokritov, B. Bartenlian, C. Chappert, D. Decanini, F. Rousseaux, F. Carcenac: J. Appl. Phys. **81**, 4993 (1997).

[24] F. Rousseaux, D. Decanini, F. Carcenac, E. Cambril, M.F. Ravet, C. Chappert, N. Bardou, B. Bartenlian, and P. Veillet, J. Vac. Technol. B 13 2787 (1995).
[25] B. Hillebrands, Rev. Sci. Instr. 70, 1589 (1999).
[26] S.O. Demokritov and E. Tsymbal, J. Phys.: Condens. Mater. 6, 7145 (1994).
[27] B. Hillebrands, Brillouin light scattering from layered magnetic structures, in: *Light Scattering in Solids* VII, G. Güntherodt, M. Cardona (eds.), Spinger, Heidelberg, in press.
[28] S.O. Demokritov and B. Hillebrands, J. Mag. Mag. Mag. 200 (1999) in press.
[29] C. Kittel, Phys. Rev. 73, 155 (1948).
[30] R.I. Joseph and E. Schlömann, J. Appl. Phys. 36, 1579 (1965).
[31] P. Grünberg, C.M. Mayr, W. Vach, J. Mag. Mag. Mat. 28 319 (1982).